

Non-woven materials for cloth-based face masks

inserts: Relationship between material properties

and sub-micron aerosol filtration

Leigh R. Crilley*, Andrea A. Angelucci, Brian Malile, Cora J. Young, Trevor C. VandenBoer,
and Jennifer I. L. Chen*

Department of Chemistry, York University, Toronto, ON, Canada

*Corresponding Authors: jilchen@yorku.ca, lcrilley@yorku.ca

KEYWORDS: mask material, non-woven, filter, aerosol filtration, infectious respiratory disease,
community transmission, air pollution, SARS-CoV-2

Abstract

Current guidance by leading public health agencies recommends wearing a 3-layer cloth-based face mask with a middle non-woven material insert to reduce the transmission of infectious respiratory viruses like SARS-CoV-2. In this work we explore the material characteristics for a range of readily available non-woven materials and their sub-micron particle filtration efficiency (PFE), with the aim of providing evidence-based guidelines for selecting appropriate materials as inserts in cloth-based masks. We observed a wide range of ideal PFE for the tested non-woven materials, with polypropylene, Swiffer and Rayon/polyester blend providing the highest PFE and breathability. Our results suggest that materials comprising loose 3D fibrous webs (e.g. flannel, Swiffer and gauze) exhibited enhanced filtration efficiency compared to compressed counterparts. Common modifications to fabrics, such as water-resistant treatment and a sewn seam were also investigated. Overall, we demonstrate that adding an appropriate non-woven material as an insert

1 filter can significantly improve the performance of cloth-based masks, and there exist suitable
2 cellulose-based alternatives to polypropylene.

3 **Environmental significance statement (<120 words)**

4 The widespread use of face masks has previously been adopted by those living in megacities and
5 low- or middle-income countries to combat the effects of air pollution. The identification of
6 infectious respiratory aerosols in the same size range as aerosols in air pollution, coupled with
7 supply chain disruption in the pandemic, highlights the need for guidelines in face mask material.
8 Reusable cloth-based masks are environmentally responsible alternatives to disposables. In this
9 work non-woven material inserts to improve nanoscale filtration efficiency of cloth-based masks,
10 and further their lifetime, are explored. We employ industry filtration testing standards to identify
11 suitable materials. A greater uptake of mask use will reduce the transmission of sub-micron
12 respiratory aerosol and reduce exposure to atmospheric aerosol pollution.

13 **INTRODUCTION**

14 Scientific evidence supports the spread of severe acute respiratory syndrome coronavirus
15 2 (SARS-CoV-2) from exposure to infectious viral aerosol (0.10 to 10 μm) emitted from the human
16 respiratory tract in air,¹ consistent with case studies of the spread of influenza (H1N1) and SARS-
17 CoV in indoor environments, such as restaurants, call centres, and aircraft.²⁻⁶ Consequently, the
18 World Health Organization (WHO) and many public health authorities recommend wearing a
19 mask or face covering in public spaces to reduce transmission of SARS-CoV-2 during the
20 pandemic.

21 A healthy individual respires aerosol of a similar size during speaking or breathing, but up
22 to an order of magnitude more when speaking, as measured by number of aerosols per cubic
23 centimeter of air.^{7,8} The fate of aerosols emitted by people depends largely on their size.⁹ Coughing

1 and sneezing typically release larger respiratory droplets ($>5\text{ }\mu\text{m}$ in diameter) that can affect the
2 immediate area ($\sim 2\text{ m}$) on the order of minutes, followed by the droplets settling to surfaces.
3 Meanwhile the smaller aerosols ($<5\text{ }\mu\text{m}$) typically released by breathing or speaking can travel
4 tens of meters and remain entrained in air for hours due to their low mass, furthering the area of
5 infection risk.^{7,10,11} In indoor environments, aerosols with diameter less than $2.5\text{ }\mu\text{m}$ can remain
6 suspended for up to 10 hours.¹² It was observed that SARS-CoV-2 remains viable in aerosols after
7 3 hours of suspension in air,¹³ and a recent work reported viable virus in airborne aerosol of 0.25
8 to $0.5\text{ }\mu\text{m}$.¹⁴ The highly transmissible new variants of SARS-CoV-2 have raised alarms of airborne
9 risks. There is growing evidence of individuals being exposed to infective aerosols occurring at
10 distances beyond 2 meters from an infected person in enclosed spaces,¹⁵ and past reports of SARS
11 outbreaks in high-rise buildings suggested aerosols can traverse between vertically aligned
12 apartments through connected drainage pipes and vents.^{16–18} A greater preparedness in cataloguing
13 properties of mask materials, including their sub-micron aerosol filtration efficiency, may allow
14 rapid policy adjustments and recommendations by health agencies for personal protection. In the
15 current work, we use the term aerosol throughout but note within the literature the term particle is
16 also used synonymously.

17 The shortage of commercial masks in the early onset of the pandemic has inspired do-it-
18 yourself movements for cloth masks. These can be readily sewn, and the improved comfort and
19 personalization offers resilience against mask fatigue. Although cloth-based face coverings
20 provide less protection than medical-grade or N95 masks, they are intended for use in different
21 settings. Medical-grade masks must protect the wearer in high-risk settings (e.g. hospital), while
22 cloth masks are viable alternatives in reducing community transmission without depleting precious
23 personal protective equipment from health workers.¹⁹ Recent modeling results demonstrate that

community mask use provides a high return in reducing the duration and amplitude of future waves of SARS-CoV-2 transmission,²⁰ with work demonstrating superior performance of masks over face shields in limiting aerosol emission in a human cough simulator.²¹ Increasing the effectiveness of cloth-based masks with broadly accessible non-woven inserts will realize further gains.

Due to the well-established risks associated with air pollution and atmospheric fine particles (PM_{2.5})²², reducing personal exposure with cloth-based face masks is increasingly popular in countries such as South and East Asia that suffer from poor air quality.^{23,24} There is evidence that wearing a face mask can reduce some of the harmful effects of air pollution exposure, but it remains unclear what level of reduction is required to obtain any benefits.^{25,26} There has been limited work on the ability of cloth-based face masks to filter ambient aerosol, with studies generally finding their overall efficacy to be reduced owing to poor fit and design. Shakya et al.²⁷ used sub-micron diesel exhaust aerosol as a proxy for air pollution and found the filtration efficiency of commercial cloth-based face mask varied between 16-57%, with the variance attributed to the design and materials used. With sub-micron ambient aerosol thought to be more toxic than larger aerosol,²⁸ methods to increase the effectiveness of cloth-based face masks to filter sub-micron aerosol can also be applied to reduce personal exposure to air pollution.

Several works examined different materials for cloth masks or face coverings. Most of the research focused on testing the filtration efficiency of larger aerosol sizes ($>1\ \mu\text{m}$) of the materials because this size fraction covers the majority of aerosols emitted in human breathing that may contain viable infectious virus.²⁹ Pan et al.²¹ observed increasing filtration efficiency with increasing aerosol size, consistent with theory.³⁰ Most materials had filtrations of $>50\%$ at $2\ \mu\text{m}$ and $>75\%$ at $5\ \mu\text{m}$. Similarly, Rogak et al.³¹ found that nearly all materials tested removed aerosols $>5\ \mu\text{m}$, though the filtration efficiency of $1\text{-}5\ \mu\text{m}$ aerosols for common fabrics varied considerably,

1 with the difference in filtration performance partly explained by material structure. Theoretical
2 prediction of filtration efficiency is related to the packing density of the fibers, the mat thickness,
3 diameter of the fibers and the single fiber efficiency.³⁰ This relationship, however, is not readily
4 applied to fabrics because the wide range of weaves and structures of yarns where fibers are not
5 all perpendicular to the flow. Besides filtration efficiency, the flow impedance of the material, a
6 measure of its breathability, is crucial when considering the thermal comfort of face masks.^{32–35}
7 Increasing the number of layers of material results in an increase in filtration efficiency, yet reduces
8 the breathability.³⁴ Hence, when choosing materials for multi-layer face masks both variables need
9 to be considered. It is important to note that the efficacy of a face mask not only depends on its
10 ideal filtration properties, but to a large extent on the fit of the face mask. Small leaks (1-2% by
11 area) can lead to notable decreases in filtration efficiency of up to 66 % for aerosols less than 5
12 μm .^{32,36} Several works have shown that cloth-only layers do not provide adequate blocking of sub-
13 micron aerosols.^{37,38} Accordingly, the WHO and other public health agencies are recommending
14 a 3-layer combination comprising a middle non-woven material. To this extent, some studies
15 examined vacuum bag³² and furnace filters, such as HEPA and MERV-13.^{21,34,39} Although these
16 commercial filters are highly effective for blocking sub-micron aerosol, they are not intended as
17 single-use and would require disassembling of the product by the consumer.

18 Herein, we present a study of non-woven materials that are readily available, low-cost and
19 easily cut for use as insert filters in cloth-based masks. Instead of performing a blanket survey
20 of tens or hundreds of products in the market, we applied the knowledge of manufacturing process,
21 fiber blend and desirable characteristics to guide our selection. We investigated the ideal filtration
22 efficiency of sub-micron sized aerosols, breathability and materials properties. We also examined
23 the effects of common modifications to fabrics including the application of water-resistant

treatment and the presence of a seam. With the increasing knowledge on the likelihood of viral transmission through aerosols, our study aims to complement existing work, bridge the gap of fundamental science of cloth-based masks, and help provide evidence-based guidelines on the selection of material for mask design. Our findings can be more broadly implemented in the reduction of other environmental aerosol exposures of concern, such as those constituents in sub-micron atmospheric aerosols identified as carcinogens.⁴⁰

METHODS

Materials

Materials were purchased from local shops and online, where the public would be likely to obtain material. Prima cotton (used in crafts), woven cotton (for apparel), interfacing and polypropylene were purchased from Fabricland, Canada. The microfiber fabric was a bedding sheet procured from Amazon. The baby wipe was Pamper's Sensitive wipe (Walmart), and the hydroentangled wipes (Grainger) were Berkshire Durx570 (cellulose/polyester), Berkshire ValuClean Plus (Rayon/polyester) and ACL staticide heavy duty. Gauze pad was Life brand (Shopper's drugmart). Nikwax Cotton Proof and TX Direct Spray-on water-resistant treatments (Amazon) were applied to the fabrics according to manufacturer's instruction. The blue disposable mask was Formedica brand and the green disposable mask was from Charmed Biotechnology Co., Ltd., Taiwan.

Materials Characterization

Scanning electron microscopy (SEM)

A FEI Quanta 3D dual-beam scanning electron microscope equipped with an Everhart-Thornley detector (ETD) operated under high vacuum and 25 kV accelerating voltage was used to obtain the images. Samples were sputtered with Au prior to imaging.

Diffuse reflectance

A Perkin Elmer Lambda 950 UV-Vis-NIR spectrophotometer equipped with a 150-mm integrating sphere was used to measure the diffuse reflectance of the samples.

Optical microscopy

Reflectance images were captured using a Nikon TE-2000U inverted microscope with a 10x objective and a Jenoptik CCD camera.

Water contact angle

A homemade setup comprising a camera, a sample stage and an illumination light source was used to capture the image of water droplet on the hydrophobic materials. The contact angle was analyzed using ImageJ.

Aerosol experiments

The methodology for the aerosol filtration efficiency testing was adapted from that proposed by Schilling et al.⁴¹ for screening filtration properties of face masks. We chose to use NaCl as the test aerosol, as it has been widely used in regulatory testing of face masks.⁴² NaCl aerosols were generated by flowing 2 L/min of N₂ through a nebulizer containing a solution of 2% w/w NaCl in deionized water. The aerosol flow was then mixed with 1 L/min of dry zero air to achieve a total flow of 3 L/min. A flow rate of 3 L/min was chosen to mimic a moderate-heavy breathing rate (30 L/min),⁴³ when scaled to the area of material tested relative to a standard surgical mask (ca. 167 cm²);⁴¹ it corresponded to an air velocity of 3 cm s⁻¹ which is within the recommended test range of 0.5-25 cm s⁻¹ from ASTM F2299. A subset of material combinations was also tested at a lower flow rate of 1.5 L/min, representative of resting breathing rate (e.g. sitting).⁴³ The generated aerosols had an average geometric mean diameter of 67.2 ± 9.6 nm with

a geometric standard deviation of 2.30. Before each material was tested the NaCl aerosol flow was equilibrated for about an hour.

Aerosol filtration efficiency testing

NaCl aerosols with a diameter from 14-736 nm were analyzed with a TSI Scanning Mobility Particle Sizer (SMPS); comprising a TSI 3080 Electron Classifier (EC), a TSI 3081 Long Differential Mobility Analyzer (DMA), and a TSI 3775 Condensation Particle Sizer (CPC). The SMPS was run using a 3 L/min sheath flow and a 0.3 L/min aerosol flow with a scan time of 5 minutes per sample. A stainless steel 47-mm diameter filter holder was fitted between the aerosol flow and the SMPS to house materials during testing. Prior to testing, materials were conditioned for at least 24 hours at 38 °C and 85 % RH to mimic human respiration and then cut into 47-mm diameter discs. All lines that carried aerosol were either ¼ inch O.D. conductive or stainless-steel tubing with a total line length of ~1 m and all fittings used were ¼ inch stainless steel Swagelok. Aerosols were not neutralized before the test material which would not be a significant source of error given that similar aerosol filtration efficiencies have been demonstrated for charged and neutralized particles.³² The water content of the aerosol output was controlled by diluting the aerosol flow (2 L/min) using zero air (0%RH, 1 L/min) resulting in effective RH of 66%.

A detailed description of the material testing regime can be found in the Supporting Information. Briefly, each material was tested three times, with a new sample of material used for each test. For each sample test, three SMPS scans were recorded. Prior to and after each sample test (ca. every 20 mins), measurements of the nebulizer output with an empty filter holder were taken to monitor the variability in the test aerosol output. These negative control measurements were performed to ensure consistent test aerosol output, and co-efficient of variance (CV) of aerosol output in terms of number concentration per size bin was typically below 10% (See Figure

S1). Any sample test where the average CV in particle number concentration per size bin for the pre- and post-material tests was greater than 10% were retested. The filter holder and SMPS impactor were cleaned thoroughly using a damp Kimwipe between negative control and material tests to ensure no bias from a buildup of NaCl.

Material impedance testing

For each conditioned material, the pressure drop across the material was measured to assess the breathability of the material. The experimental set up was similar to the filtration study, except that there was no aerosol added to the flow. Thus, the nebulizer was removed from the setup. The pressure differential across the material was measured using a TPI SP620 Smart Probe (0.5 Hz) connected upstream and downstream of the filter holder for 2 minutes per material, with a 5-minute empty filter holder negative control conducted before each set of tests to assess the pressure drop caused by the filter holder alone.

Data analysis

As the test aerosol output was consistent throughout a given experiment, aerosol filtration efficiency was calculated for a tested material using the average aerosol number concentrations for the measurement (C_M , # particles cm^{-3}) and corresponding empty filter holder (C_E , # particles cm^{-3}) measurements according to Equation 1. More specifically, this equation was used determine the PFE as function of aerosol size, where the PFE was calculated for each size bin measured by the SMPS.

$$PFE (\%) = 100 * \left(1 - \frac{C_M}{C_E}\right) \quad (1)$$

Equation 2 provides an example of more broadly explored PFE for larger aerosol fractions, such as those with diameters >100 nm.

$$PFE (\%) = 100 * \left(1 - \frac{\sum_{>100nm} C_M}{\sum_{>100nm} C_E}\right) \quad (2)$$

The PFE for aerosol size fractions 100-300 nm, 300-750 nm and <100 nm were calculated similarly using Equation 2. The breathability of each material was evaluated using the impedance (I, mbar/(cm/s)) calculated from measured pressure difference across the material (Equation 3):

$$I = (\Delta P_M - \Delta P_E) \times \frac{A}{V} \quad (3)$$

Where ΔP_M and ΔP_E are the measured pressure difference (mbar) for the material sample and empty filter holder, respectively and A is the area of the material (cm²) and V the flowrate (cm³ s⁻¹). The Quality Factor (QF), a commonly used metric to evaluate overall material performance perceived by wearers and quantified experimentally, is a function of both the filtration efficiency and breathability.³⁴ QF was determined as per WHO guidelines,⁴⁴ according to Equation 4:

$$QF = \frac{-\ln(1 - \frac{PFE_{min}}{100})}{\Delta P} \quad (4)$$

Where PFE_{min} is the minimum PFE observed for each material over the entire aerosol size range measured.

RESULTS AND DISCUSSION

Material characterization

We examined four cotton-based fabrics and several different types of non-woven materials. The woven fabrics include Prima cotton (used in crafts), woven cotton (used in apparel), flannel and microfiber sheet. Previous studies have provided the knowledge on the properties of woven fabrics in relation to the filtration of droplets.^{31,34,37,45} In this work, we examine common modifications that may be applied to the fabrics and focus on investigating various non-woven

1 materials that can serve as filters to help guide the construction of 3-layer masks recommended
2 recently by WHO and Government of Canada. The non-woven materials include consumer
3 products such as sew-in interfacing, polypropylene, baby wipe and Swiffer. We also examined
4 three industrial wipes comprising hydroentangled fibers of different compositions:
5 cellulose/polyester, Rayon/polyester and electrostatically charged cellulose/polyester (ACL
6 staticide). A Rayon/polyester gauze was also examined. The non-woven materials manufactured
7 using different methods exhibit different densities and morphologies of fibers. The photographs of
8 the materials are shown in Figure S2. We measured the basis weight, optical diffuse reflectance,
9 and water contact angle (if applicable) of the materials, as summarized in Table 1. The basis weight
10 provides information on the density of fibers per area and correlates with the diffuse reflectance
11 for the non-woven materials (Figure S3); however, the trend is absent for fabrics. The scanning
12 electron microscopy and optical reflectance images of the materials are shown in Figure 1 and
13 Figure S4.

14 The non-woven materials were selected based on their availability, practicality, and
15 properties such as hydrophobicity and electrostatics that have been suggested to be desirable in
16 filters. The interfacing material comprising dry-laid polyester fibers exhibits high porosity (seen
17 in Figure S3a) and low optical reflectivity. Figure 1a shows the SEM image of the polypropylene
18 material comprising spunlaid fibers that are thermally bonded.⁴⁶ Swiffer, shown in Figure 1b,
19 consists of polyester/polypropylene fibers that form an open three-dimensional fibrous web which
20 is electrostatically charged to attract and trap particles. Figures 1c-f show the microscopic
21 structures of the wipes; interestingly, longitudinal grooves along the fibers were observed in the
22 Rayon/polyester blend (Figure 1d) and to a lesser extent in the baby wipe (Figure 1c). In contrast,
23 the material containing cellulose showed flat ribbons intermixed with cylindrical fibers (Figure

1e). Although the industrial wipes (Figure 1d – f) were all produced using hydroentanglement, the morphology varies greatly depending on the composition of the fibers.

Aerosol filtration efficiency of single layer materials

For each material, we tested the ideal aerosol (particle) filtration efficiency (PFE) of NaCl aerosols of 14 nm to 736 nm in size. A schematic of the setup is shown in Figure 2. Figure 3 shows the PFE as a function of aerosol size for the different materials. The PFE is nearly flat above 300 nm and increases exponentially with decreasing aerosol size below ~200 nm. This observation is consistent with previous work, where the filtration mechanism transitions from inertia- or impact-based capturing of large droplets to electrostatic attraction for the submicron-sized aerosols.⁴⁷ Smaller aerosols (i.e. <200 nm) were efficiently captured due to their Brownian motion delivering them to the fibre surfaces.

Figure 3a shows the PFE vs aerosol size for the fabrics, where the comparative performance of flannel being greater than woven cotton is consistent with previous reports.^{32,34,37} Flannel has directionally oriented raised fibers from the weave (i.e. nap) and is more effective at filtration than plain woven cotton. The microfiber fabric we tested is light weight and did not show improved performance compared to woven cotton despite the high thread count (1080 TPI). Studies have shown that thread count did not correlate with filtration efficiency because fabrics with higher thread count might consist of thinner fibers which have low single fiber efficiency.³² For comparison, we tabulated the PFE of aerosols of different size ranges and summarized the overall PFE of >100 nm particles (i.e. 100 – 750 nm; Table 2). We set 100 nm as our cut-off because the size of the virus is ~100 nm, below which fragments of the viral components are considered non-infectious. The virus would be present in aerosol with dried salts and other components of respiratory fluid, thereby the diameter of potential viable aerosols would be above this 100 nm

limit. Thus, a PFE >100nm is a conservative (or worst-case) estimate of material performance. PFE data for aerosol less than 100 nm, also known as ultra-fine particles (UFP), are included to provide a deeper insight into the materials' performance. Emerging evidence suggest UFP in polluted ambient air may have enhanced toxicity compared to larger aerosols.²⁸ Herein the overall PFE discussed refers to size >100 nm unless otherwise noted. We observed a low PFE of 6.9 % by woven cotton, 4.2 % by microfiber and 15.6 % by flannel.

We then examined common modifications to the fabric, such as a seam that can be present in certain mask designs. Using flannel as the example, we measured statistically similar PFE of >100 nm for fabric with (20.7 %) and without (15.6 %) a seam ($p > 0.05$). In contrast, for <100 nm particles where filtration by diffusion is the dominant mechanism, the PFE of flannel with seam (52.2 %) is significantly higher than without a seam (40.9 %, $p < 0.01$). The increase may have arisen from the added amount of fabric at the seam (~25 % for the tested area of 14.5 cm²). The results show that leakage through the seam was minimal and should not deter the design of a well-fitted mask. We examined the application of a water-resistant product to yield hydrophobic fabrics. Based on the properties of disposable masks and public health guidelines, having a hydrophobic outer layer may be beneficial for enhancing filtration efficiency. We observed a relative increase of 52 % in PFE when the flannel was treated with the water-repellent product (denoted as WR-flannel), from 15.6 % to 23.7 % ($p < 0.01$). Figure S4 shows the PFE distributions of flannel with different modifications. Nevertheless, with two layers of woven fabrics, the PFE ranged from 12.6 % for woven cotton to 30.5 % for flannel, outlining the ineffectiveness of cloth-based face coverings against sub-micron aerosols.^{37,38} Thus, it is desirable to include a more effective filtration material in layers, particularly for use in the moderate to heavy flow regime expected under moderate physical exertion.⁴³

Relationship of material properties and PFE

Figure 3b,c show the PFE vs aerosol size for the non-woven materials. For consumer products, polypropylene and Swiffer performed comparably with overall PFE of 21.2 and 22.3 %, respectively (Table 2). On the other hand, the dried baby wipe showed 8.0 % PFE and the interfacing polyester material was completely ineffective (PFE \sim 0%). We note that the breathability of Swiffer is four times higher than polypropylene, with an impedance of 0.01 vs 0.04 mbar/(cm/s). The lower impedance of Swiffer compared to polypropylene leads to its higher quality factor, which is a combined measure of material breathability and PFE. Three hydroentangled wipes were investigated because the manufacturing process yields mechanically strong and interlocked fibers; the increase in fiber packing density was hypothesized to enhance PFE.

Figure 3c shows the PFE distribution of the Rayon/polyester, cellulose/polyester and ACL staticide (compositionally also cellulose/polyester) wipes. The ACL staticide exhibited PFE of 36.1 %, followed by Rayon/polyester wipe of 26.6 %, and cellulose/polyester of 9.2 %. The ACL staticide wipe has the highest basis weight of all wipes and is electrostatically charged. It outperformed polypropylene in terms of PFE, however, it was also the least breathable out of all single-layer materials. On the other hand, the Rayon/polyester wipe (NW6) exhibited similar PFE performance as polypropylene but had a lower impedance (0.01 vs 0.04 mbar/(cm/s)) and hence a high quality factor of 44.7. Because the cellulose-based wipes are highly sorbent, we hypothesized that a prolonged exposure to moisture, such as the pre-conditioning step we employed, may influence the properties of the material. We tested the Rayon/polyester wipe without pre-conditioning (NW6U) and found a higher PFE at 38.9 % compared to that with conditioning at 26.6 %; a change in the impedance was also detected (0.01 vs 0.03 mbar/(cm/s) with and without

conditioning, respectively). The statistically different PFE ($p < 0.05$) suggests that prolonged use and exposure to respiratory droplets may diminish the PFE of sorbent materials. Notably, the hydroentanglement process did not yield consistently high PFE across the different materials, suggesting that chemical composition, microstructure and other materials properties are important factors and control the single fiber efficiency.^{46,48} We hypothesize that the superior sorbency of the Rayon/polyester blend (439 mL/m²) and its longitudinal grooves on the fiber morphology, which yielded high surface-area-to-volume ratio, may have led to a high single fiber efficiency.

As such, we tested another material comprising Rayon/polyester blend – a gauze pad. At 3-ply (i.e. 3 layers), the PFE shown in Figure 3e was extremely high (at 78.8 % for >100 nm particles), while the impedance (0.02 mbar/(cm/s)) was comparable to other non-woven materials. Gauze can be an effective filter material that is breathable and widely accessible to the general public, though we caution that there exist variations of gauze which may have different weaves and pore sizes. The gauze we investigated was spunlaced non-woven rather than woven, with loose fibers that rise between the pores (Figure S4h). Our results suggest that materials comprising loose 3D fibrous webs (e.g. flannel, Swiffer and gauze) exhibit enhanced filtration efficiency compared to compressed counterparts, in line with previous finding that the better material structures expose individual fibers to the flow.³² Figure S6 summarizes the PFE of woven and non-woven materials with respect to the optical reflectance.

Aerosol filtration efficiency of multilayer materials

Next, we investigated the PFE of multilayer materials comprising cotton fabrics with or without selected non-woven materials as the filter. Figure 3d shows their PFE vs aerosol size. As discussed above, a bilayer of woven or Prima cotton yielded low PFE. With two layers of flannel, the PFE was 30.5 %. Upon adding polypropylene, Swiffer, or Rayon/polyester wipe as the filter

in between the flannel (Figure 3e), the PFE increased to 49.0 %, 40.4 % and 48.7 % respectively (corresponding to combinations M4 – M6 listed in Table 2). Figure 4 summarizes the PFE for two aerosol size bins to outline the effects of layering. The addition of these selected non-woven materials as a filter boosted the ideal aerosol blocking efficiency by a magnitude of ~20 %. As the percentage of filtration of the i th layer is the PFE of the i th material multiplied by the percentage of unfiltered particles from the previous ($i-1$) layer, an overall PFE of multilayer composition can be calculated according to:³²

$$PFE_{total} = 1 - (T_{L1} \times T_{L2} \times \dots) \quad (5)$$

where T_{Li} is the transmission of the i th layer. Using equation 5, the predicted PFE of M4, M5 and M6 are 44, 49 and 48 % respectively, close to the experimental values (see Table S2). The impedance of multilayer combinations, on the other hand, is the sum of the individual layers.³² Hence increasing the number of layers (e.g. beyond 3 layers) may not provide a substantial improvement in PFE that would justify the decrease in breathability. Additionally, we tested the PFE of M4 and M5 at a low flow rate (1.5 L/min), representative of resting breathing rate.⁴³ We observed an increase in PFE by ca. 6% for both material combinations, to 55.6 % and 46.7 % for M4 and M5, respectively. This observation agrees with previous findings for submicron aerosols³² and is due to the change in residence time of aerosols within the material.

For comparison, we tested the PFE of two disposable masks (referred to as blue and green, based on their colors). We tested inward and outward effectiveness with aerosols impinging on the outer layer vs the inner layer to examine the protection of the masks for and from the wearer. The PFE of the disposable masks are shown in Figure 3f. Interestingly, the green mask exhibited a difference between the two sides of the mask (84.3 % vs 94.1 %) while the blue mask performed with ~95 % PFE in both directions. The differences in performance between the masks reflect their

construction: the blue mask consisted of spunbond polypropylene/electrostatic melt-blown fibers/spunbond polypropylene where the terminal layers were made of the same material. The water contact angles of the two sides of the blue mask were comparable (i.e. 125.7 vs 121.4 degrees, Table 1). The green mask, however, was constructed to be more breathable as the manufacturer referenced a composition of spunbond polypropylene (outer layer), electrostatic melt-blown fibers (middle) and a breathable inner layer. The impedance of the green mask (0.07) was observed to be lower than that of blue mask (0.11). We observed the inner layer of the green mask to have similar properties as the interfacing material, though its composition is unknown. The water contact angles of the outer and inner layer of the green mask were 119.4 and 102.5 degrees, respectively. The different wetting behavior contributed to the difference in PFE when measured in forward vs reverse directions. It suggests that some disposable masks are designed to primarily protect the wearer, and it is important to wear them correctly.

Ranking of tested materials

We ranked the PFE for all tested materials in Figure 5 and summarized the results of impedance vs PFE in Figure 6, where a high PFE and low impedance are desirable (i.e. lower right quadrant of the graph). In single layer materials (Figure 6a), non-woven materials such as polypropylene, Swiffer and hydroentangled Rayon/polyester wipe were effective filters with high breathability (i.e. low impedance). Generally, hydroentangled materials had higher PFE than dry-laid or spunlaid non-woven materials such as interfacing and baby wipe.

The multilayer combinations tested had a similar impedance as the disposable mask but with varied and lower PFE (Figure 6b). The WHO recommends cloth-based masks have a QF greater than 3. All of the 3-layer combinations tested here exceed these WHO guidelines and would be a suitable alternative to disposable masks for use in low-risk settings. Of the tested multi-layer

material combinations, 3-layer gauze had the highest PFE, similar to the tested disposable masks (Fig 6b). Notably, the suitable non-woven materials identified in our study, such as Swiffer, hydroentangled Rayon/polyester wipe and gauze, cost 0.03 – 0.09 USD per insert (estimated for an area of 160 cm²).

CONCLUSION

In summary, we examined the properties of a range of non-woven materials and their sub-micron aerosol filtration efficiency (PFE) to provide evidence-based guidelines for selecting cloth-based mask inserts. Different compositions of fibers yielded different fiber morphologies, and the manufacturing processes produced various fibrous web structures and mat densities. Fabrics and non-woven materials comprising raised or loose fibers, such as flannel and gauze, were found to exhibit enhanced filtration efficiency compared to flattened counterparts, such as regular woven cotton and Rayon/polyester wipe, respectively. Electrostatically charged non-woven materials were effective filters, with Swiffer, which exhibits a three-dimensional porous fibrous structure, offering high breathability. These materials are cheap and can be readily cut by the public to be used as filter inserts, in comparison to other works that recommended commercial filters such as MERV 13, vacuum bags or HEPA furnace filters. Of the different cellulose-based fibers, the Rayon/polyester blend performed equally or better than polypropylene; however, the filtration efficiency of sorbent materials was affected by prolonged exposure to moisture. Notably, common consumer products such as sew-in interfacing and dried baby wipe were ineffective at filtering sub-micron aerosols. We also showed that introducing water-repellency in fabrics can increase the filtration efficiency, and the presence of a seam did not deteriorate the performance of the flannel fabric. The impedance and submicron PFE of a multi-layer mask construction with a selected material insert can be predicted with a reasonable accuracy based on the measured values of

materials in each individual layer. Beyond addressing the need of the current pandemic, the knowledge on the selection of materials for cloth-based masks will help provide guidance on personal protection against air pollution with similar sized aerosols of concern.

Acknowledgements

This work is supported by a York University COVID-19 research fund and NSERC Discovery grants and COVID-19 supplements to TV, CY, and JC. AAA received funding from Enbridge Graduate Student Award, Dr. Ralph Nicholls Graduate Scholarship and Charles Hantho Award. The authors thank Arthur Chan for the loan of the stainless-steel filter holder and Dr. Jaklewicz for assistance with SEM.

Author contributions

Conceptualization of study led by JC with input from TV and CY. Aerosol testing methodology developed by LC; aerosol investigation, data collection and formal analysis by LC and AA. Materials characterization and analysis performed by BM and JC. Funding secured by CY, TV and JC. Writing original draft by LC, TV and JC, and review and editing by all authors.

Conflict of interest

The authors declare no conflict of interest.

Supplementary material

Supplementary material available. See doi:XXXX.

References

- 1 J. Gralton, E. Tovey, M. L. McLaws and W. D. Rawlinson, *J. Infect.*, 2011, **62**, 1–13.
- 2 H. Lei, Y. Li, S. Xiao, C.-H. Lin, S. L. Norris, D. Wei, Z. Hu and S. Ji, *Indoor Air*, 2018,
- 3 **28**, 394–403.
- 4 S. Y. Park, Y.-M. Kim, S. Yi, S. Lee, B.-J. Na, C. B. Kim, J. Kim, H. S. Kim, Y. B. Kim,
- 5 Y. Park, I. S. Huh, H. K. Kim, H. J. Yoon, H. Jang, K. Kim, Y. Chang, I. Kim, H. Lee, J.
- 6 Gwack, S. S. Kim, M. Kim, S. Kweon, Y. J. Choe, O. Park, Y. J. Park and E. K. Jeong,
- 7 *Emerg. Infect. Dis. J.*, 2020, **26**, 1666.
- 8 J. Lu, J. Gu, K. Li, C. Xu, W. Su, Z. Lai, D. Zhou, C. Yu, B. Xu and Z. Yang, *Emerg.*
- 9 *Infect. Dis.*, 2020, **26**, 1628–1631.
- 10 F. Zhang, Y. Wang, J. Peng, L. Chen, Y. Sun, L. Duan, X. Ge, Y. Li, J. Zhao, C. Liu, X.
- 11 Zhang, G. Zhang, Y. Pan, Y. Wang, A. L. Zhang, Y. Ji, G. Wang, M. Hu, M. J. Molina
- 12 and R. Zhang, *Proc. Natl. Acad. Sci. U. S. A.*, 2020, **117**, 3960–3966.
- 13 S. L. Miller, W. W. Nazaroff, J. L. Jimenez, A. Boerstra, G. Buonanno, S. J. Dancer, J.
- 14 Kurnitski, L. C. Marr, L. Morawska and C. Noakes, *Indoor Air*, 2020, DOI:
- 15 10.1111/ina.12751.
- 16 L. Morawska, G. R. Johnson, Z. D. Ristovski, M. Hargreaves, K. Mengersen, S. Corbett,
- 17 C. Y. H. Chao, Y. Li and D. Katoshevski, *J. Aerosol Sci.*, 2009, **40**, 256–269.
- 18 C. Y. H. Chao, M. P. Wan, L. Morawska, G. R. Johnson, Z. D. Ristovski, M. Hargreaves,
- 19 K. Mengersen, S. Corbett, Y. Li, X. Xie and D. Katoshevski, *J. Aerosol Sci.*, 2009, **40**,
- 20 122–133.
- 21 L. Morawska, in *Proceedings of Indoor Air 2005: the 10th International Conference on*
- 22 *Indoor Air Quality and Climate*, Springer, 2005, pp. 9–23.
- 23

1 10 S. Asadi, N. Bouvier, A. S. Wexler and W. D. Ristenpart, *Aerosol Sci. Technol.*, 2020, **54**,
2 635–638.

3 11 L. Morawska and J. Cao, *Environ. Int.*, 2020, **139**, 105730.

4 12 W. J. Riley, T. E. McKone, A. C. K. Lai and W. W. Nazaroff, *Environ. Sci. Technol.*,
5 2002, **36**, 200–207.

6 13 N. van Doremalen, T. Bushmaker, D. H. Morris, M. G. Holbrook, A. Gamble, B. N.
7 Williamson, A. Tamin, J. L. Harcourt, N. J. Thornburg, S. I. Gerber, J. O. Lloyd-Smith, E.
8 de Wit and V. J. Munster, *N. Engl. J. Med.*, 2020, **382**, 1564–1567.

9 14 J. A. Lednicky, M. Lauzardo, M. M. Alam, M. A. Elbadry, C. J. Stephenson, J. C. Gibson
10 and J. G. Morris, *medRxiv*, 2021, 2021.01.12.21249603.

11 15 The Lancet Respiratory Medicine, *Lancet Respir. Med.*, 2020, 8, 1159.

12 16 Y. Li, S. Duan, I. T. S. Yu and T. W. Wong, *Indoor Air*, 2005, **15**, 96–111.

13 17 I. T. S. Yu, Y. Li, T. W. Wong, W. Tam, A. T. Chan, J. H. W. Lee, D. Y. C. Leung and T.
14 Ho, *N. Engl. J. Med.*, 2004, **350**, 1731–1739.

15 18 M. Kang, J. Wei, J. Yuan, J. Guo, Y. Zhang, J. Hang, Y. Qu, H. Qian, Y. Zhuang, X.
16 Chen, X. Peng, T. Shi, J. Wang, J. Wu, T. Song, J. He, Y. Li and N. Zhong, *Ann. Intern.*
17 *Med.*, 2020, **173**, 974–980.

18 19 K. A. Prather, C. C. Wang and R. T. Schooley, *Science (80-.)*, 2020, **368**, 1422–1424.

19 20 R. O. J. H. Stutt, R. Retkute, M. Bradley, C. A. Gilligan and J. Colvin, *Proc. R. Soc. A*
20 *Math. Phys. Eng. Sci.*, 2020, **476**, 20200376.

21 21 J. Pan, C. Harb, W. Leng and L. C. Marr, *medRxiv*, 2020, 2020.11.18.20233353.

22 22 P. J. Landrigan, R. Fuller, N. J. R. Acosta, O. Adeyi, R. Arnold, N. (Nil) Basu, A. B.
23 Baldé, R. Bertollini, S. Bose-O'Reilly, J. I. Boufford, P. N. Breysse, T. Chiles, C.

1 Mahidol, A. M. Coll-Seck, M. L. Cropper, J. Fobil, V. Fuster, M. Greenstone, A. Haines,
2 D. Hanrahan, D. Hunter, M. Khare, A. Krupnick, B. Lanphear, B. Lohani, K. Martin, K. V
3 Mathiasen, M. A. McTeer, C. J. L. Murray, J. D. Ndahimananjara, F. Perera, J. Potočník,
4 A. S. Preker, J. Ramesh, J. Rockström, C. Salinas, L. D. Samson, K. Sandilya, P. D. Sly,
5 K. R. Smith, A. Steiner, R. B. Stewart, W. A. Suk, O. C. P. van Schayck, G. N. Yadama,
6 K. Yumkella and M. Zhong, *Lancet*, 2018, **391**, 462–512.

7 23 K. M. Shakya, A. Noyes, R. Kallin and R. E. Peltier, *J. Expo. Sci. Environ. Epidemiol.*,
8 2017, **27**, 352–357.

9 24 J. W. Cherrie, A. Apsley, H. Cowie, S. Steinle, W. Mueller, C. Lin, C. J. Horwell, A.
10 Sleuwenhoek and M. Loh, *Occup. Environ. Med.*, 2018, **75**, 446 LP – 452.

11 25 S. Jingjin, L. Zhijing, C. Renjie, W. Cuicui, Y. Changyuan, C. Jing, L. Jingyu, X. Xiaohui,
12 R. J. A., Z. Zhuohui and K. Haidong, *Environ. Health Perspect.*, 2017, **125**, 175–180.

13 26 J. P. Langrish, X. Li, S. Wang, M. M. Y. Lee, G. D. Barnes, M. R. Miller, F. R. Cassee, N.
14 A. Boon, K. Donaldson, J. Li, L. Li, N. L. Mills, D. E. Newby and L. Jiang, *Environ.*
15 *Health Perspect.*, 2012, **120**, 367–372.

16 27 K. M. Shakya, A. Noyes, R. Kallin and R. E. Peltier, *J. Expo. Sci. Environ. Epidemiol.*,
17 2017, **27**, 352–357.

18 28 D. E. Schraufnagel, *Exp. Mol. Med.*, 2020, 1–7.

19 29 L. C. Marr, J. W. Tang, J. Van Mullekom and S. S. Lakdawala, *J. R. Soc. Interface*, 2019,
20 **16**, 20180298.

21 30 K. W. Lee and B. Y. H. Liu, *J. Air Pollut. Control Assoc.*, 1980, **30**, 377–381.

22 31 S. N. Rogak, T. A. Sipkens, M. Guan, H. Nikookar, D. Vargas Figueroa and J. Wang,
23 *Aerosol Sci. Technol.*, 2020, doi.org/10.1080/02786826.2020.1855321.

1 32 F. Drewnick, J. Pikmann, F. Fachinger, L. Moormann, F. Sprang and S. Borrmann,
2 *Aerosol Sci. Technol.*, 2021, **55**, 63–79.

3 33 A. Chauhan and R. P. Singh, *Environ. Res.*, 2020, **187**, 109634.

4 34 C. D. Zangmeister, J. G. Radney, E. P. Vicenzi and J. L. Weaver, *ACS Nano*, 2020, **14**,
5 9188–9200.

6 35 S. Kumar and H. P. Lee, *Phys. Fluids*, 2020, **32**, 111301.

7 36 W. C. Hill, M. S. Hull and R. I. MacCuspie, *Nano Lett.*, 2020, **20**, 7642–7647.

8 37 S. Rengasamy, B. Eimer and R. E. Shaffer, *Ann. Occup. Hyg.*, 2010, **54**, 789–798.

9 38 H. Lu, D. Yao, J. Yip, C. W. Kan and H. Guo, *Aerosol Air Qual. Res.*, 2020, **20**, 2309–
10 2317.

11 39 E. O’Kelly, S. Pirog, J. Ward and P. J. Clarkson, *BMJ Open*, 2020, **10**, e039424.

12 40 C. Ris, *Inhal. Toxicol.*, 2007, **19**, 229–239.

13 41 K. Schilling, D. R. Gentner, L. Wilen, A. Medina, C. Buehler, L. J. Perez-Lorenzo, K. J.
14 G. Pollitt, R. Bergemann, N. Bernardo, J. Peccia, V. Wilczynski and L. Lattanza, *J. Expo.*
15 *Sci. Environ. Epidemiol.*, 2020, DOI:10.1038/s41370-020-0258-7.

16 42 S. Rengasamy, R. Shaffer, B. Williams and S. Smit, *J. Occup. Environ. Hyg.*, 2017, **14**,
17 92–103.

18 43 N. Good, T. Carpenter, G. B. Anderson, A. Wilson, J. L. Peel, R. C. Browning and J.
19 Volckens, *J. Expo. Sci. Environ. Epidemiol.*, 2019, **29**, 568.

20 44 Advice on the use of masks in the community, during home care and in healthcare settings
21 in the context of the novel coronavirus (COVID-19) outbreak,
22 [https://www.who.int/publications/i/item/advice-on-the-use-of-masks-in-the-community-](https://www.who.int/publications/i/item/advice-on-the-use-of-masks-in-the-community-during-home-care-and-in-healthcare-settings-in-the-context-of-the-novel-coronavirus-)
23 [during-home-care-and-in-healthcare-settings-in-the-context-of-the-novel-coronavirus-](https://www.who.int/publications/i/item/advice-on-the-use-of-masks-in-the-community-during-home-care-and-in-healthcare-settings-in-the-context-of-the-novel-coronavirus-)

(2019-ncov)-outbreak, (accessed 13 December 2020).

M. Zhao, L. Liao, W. Xiao, X. Yu, H. Wang, Q. Wang, Y. L. Lin, F. S. Kilinc-Balci, A.

Price, L. Chu, M. C. Chu, S. Chu and Y. Cui, *Nano Lett.*, 2020, **20**, 5544–5552.

V. K. Midha and A. Dakuri, *J. Text. Eng. Fash. Technol.*, 2017, **1**, 126–133.

W. C. Hinds, *Aerosol technology: properties, behaviour, and measurement of airborne particles.*, 1982.

H. H. Epps and K. K. Leonas, *Int. Nonwovens J.*, 2000, **9**, 18–22.

1 TABLES

2 **Table 1.** Properties of materials.

ID	Material	Basis weight (g/m ²)	Diffuse reflectance (%)	Water contact angle (degree)
W1	Prima cotton	127.6±2.0	65.5	
W2	Woven cotton	152.5±3.4	67.0	
W3	Microfiber	95.4±3.6	69.9	
W4	Flannel	164.9±0.4	79.2	
W5	Flannel with seam			
W6	Water-resistant flannel			118.2±8.3
NW1	Interfacing light	27.0±1.2	24.2	
NW2	Interfacing medium	61.2±1.9	43.0	94.9±3.8
NW3	Polypropylene	40 ^a	32.2	117.2±7.1
NW4	Swiffer	36.6±1.8	39.0	132.2±1.3
NW5	Baby wipe	52.3±2.0	63.8	
NW6	Rayon/polyester wipe (50%/50%)	62.9 ^a	45.7	
NW7	Cellulose/polyester wipe (55%/45%)	54.6 ^a	54.8	
NW8	ACL staticide wipe (55% cellulose/45% polyester)	80.0 ^a	70.9	
M7	Blue mask			125.7±2.9 (outer); 121.4±3.0 (inner)
M8	Green mask			119.4±5.5 (outer); 102.5±2.8 (inner)
M9	Gauze (Rayon/polyester)	31.1±0.4 (1-ply)	37.0 (1-ply); 62.5 (3-ply)	

^aFrom manufacturer's specification

Table 2. Summary of aerosol filtration efficiency (PFE), impedance (I) and quality factor (QF) of materials.

ID	Material	PFE _{<100nm} (%)	PFE _{100-300nm} (%)	PFE _{300-750nm} (%)	PFE _{>100 nm} (%)	I (mbar (cm/s) ⁻¹)	QF
Woven							
W1	Prima cotton	19.2±4.0	4.3±0.7	2.0±2.1	3.4±1.3	0.04	0
W2	Woven cotton	20.8±1.9	8.3±1.2	5.2±3.3	6.9±2.1	0.04	1.9
W3	Microfiber	15.5±3.3	4.8±2.2	1.4±3.0	4.2±2.6	0.06	0.2
W4	Flannel	40.9±1.7	16.5±2.9	10.6±4.1	15.6±3.4	0.04	6.2
W5	Flannel with seam	52.2±1.7	22.5±2.2	11.7±2.5	20.7±2.4	0.06	3.9
W6	Water resistant-flannel (WR-flan.)	53.2±1.7	25.3±1.9	15.4±1.4	23.7±1.7	0.05	6.4
Non-woven							
NW1	Interfacing light	4.9±3.2	0±2.1	0±4.2	0±3.1	0.003	0.0
NW2	Interfacing medium	20.6±4.9	0.5±2.5	0±3.4	0±2.9	0.01	0.0
NW3	Polypropylene (PP)	47.0±2.9	22.5±2.5	13±4.4	21.1±3.4	0.04	5.4
NW4	Swiffer	58.5±3.0	24.8±3.6	11.3±4.6	22.3±4.1	0.01	24.7
NW5	Baby wipe	39.1±3.6	10.0±1.9	0.0±1.6	8.0±1.7	0.01	0
NW6	Rayon/polyester wipe	58.4±4.6	29.5±8.8	23.0±10.2	26.6±9.4	0.01	44.7
NW6U	Rayon/polyester wipe Uncond.	68.1±1.9	41.2±1.6	29.2±2.9	38.9±2.1	0.03	30.5
NW7	Cellulose/polyester wipe	37.6±4.6	10.6±4.0	4.1±4.9	9.2±4.4	0.03	1.8
NW8	ACL staticide wipe	65.8±0.2	37.3±1.2	31±1.7	36.1±1.4	0.12	8.6
Multilayer							
M1	Prima cotton 2 layer	22.7±1.6	9.3±2.3	6.9±2.7	8.9±2.5	0.08	2.1
M2	Woven cotton 2 layer	30.2±2.6	13.7±1.4	10.7±0.7	12.6±1.1	0.09	3.1
M3	Flannel 2 layer	65.2±0.6	31.9±0.7	22.5±0.4	30.5±0.5	0.1	6.8
M4	Flannel/PP/Flannel	88.3±1.6	52.5±1.9	35.0±2.2	49.0±2.0	0.12	8.1
M5	WR-flannel/Swiffer/Flannel	83.3±1.0	43.3±2.0	31.7±0.7	40.4±1.4	0.15	5.7
M6	Flannel/Rayon-PE/Flannel	87.3±2.3	54.4±5.2	41.5±4.5	48.6±4.9	0.09	15.9
M7	Blue mask	97.0±1.4	95.3±2.1	96.2±1.6	95.4±1.9	0.11	81.9
M7R	Blue mask (reverse)	96.9±0.7	94.8±0.7	95.5±0.3	94.9±0.5	0.11	78.4
M8	Green mask	87.4±4.6	85.4±5.8	78.3±6.4	84.3±6.1	0.07	78.6
M8R	Green mask (reverse)	95.2±0.5	97.6±0.3	75.0±1.0	94.1±0.6	0.07	114
M9	Gauze 3 layer	83.4±1.9	79.5±4.3	75.1±5.3	78.8±4.7	0.02	190

1 FIGURES

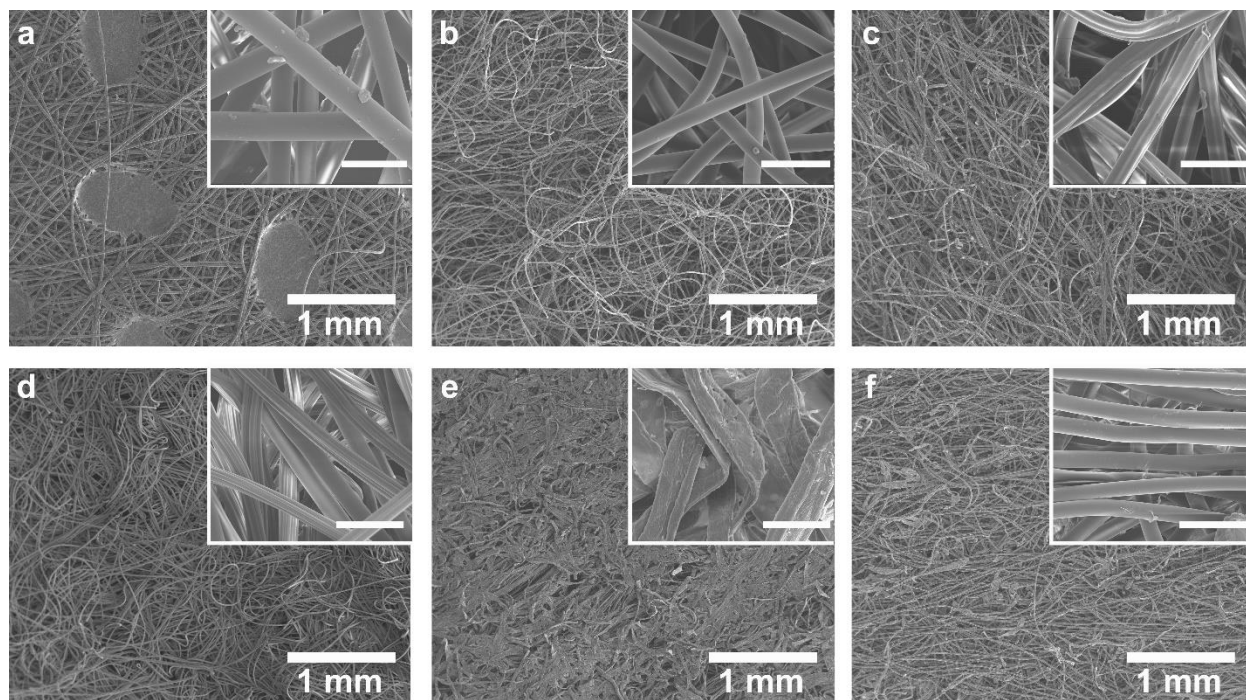


Figure 1. SEM images of non-woven materials: (a) Polypropylene; (b) Swiffer; (c) Baby wipe; (d) Rayon/polyester wipe; (e) Cellulose/polyester wipe; (f) ACL staticide wipe. Scale bar in inset: 50 μm .

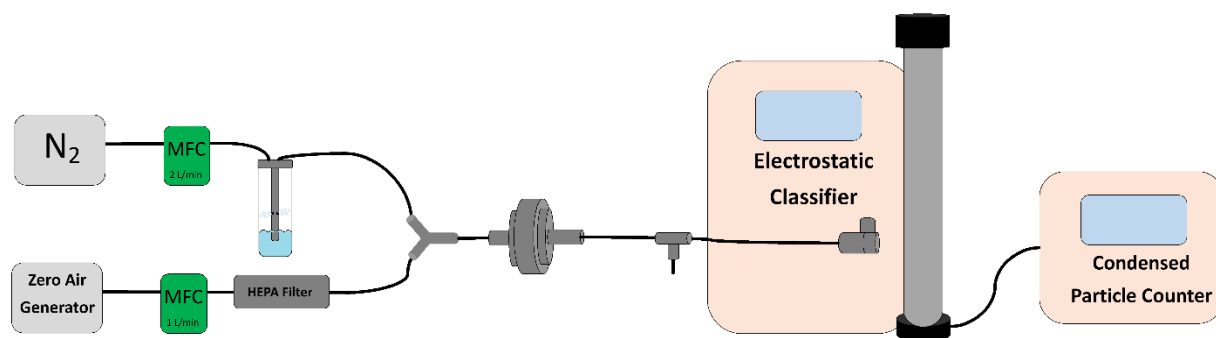


Figure 2. Schematic of the aerosol generation setup along with the SMPS detector system.

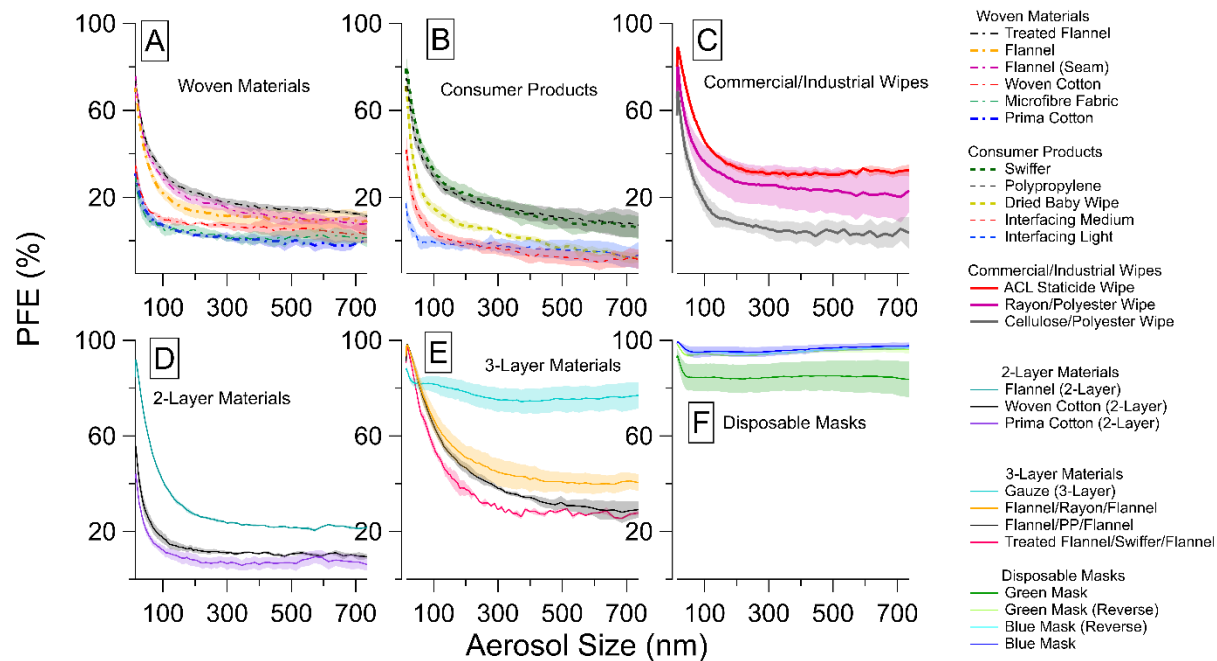


Figure 3. PFE as a function of aerosol size for all tested materials and multi-layer combinations, grouped according to material class. Variability shown is one standard deviation of the mean for the three tests.

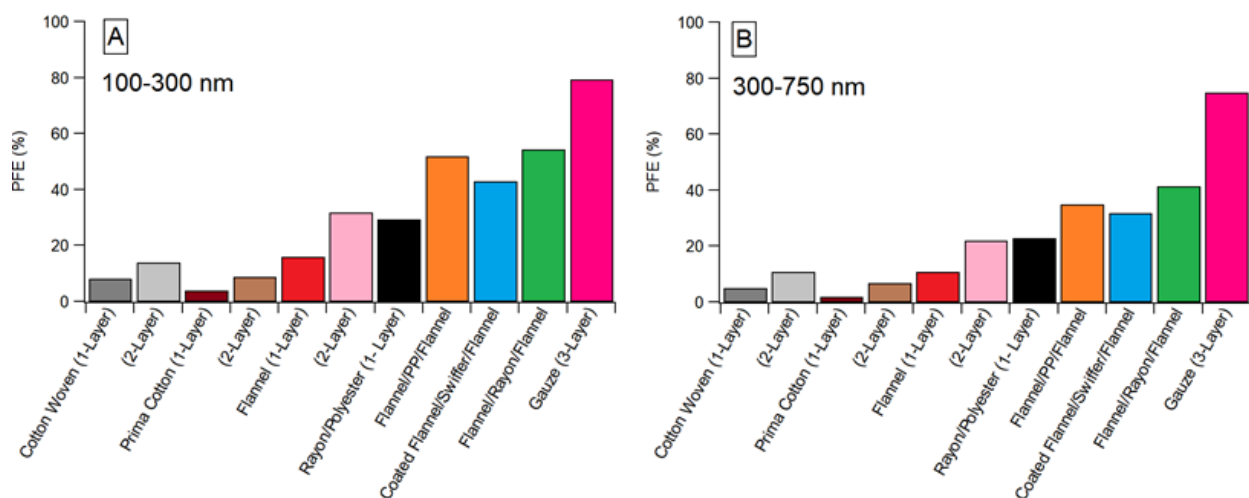


Figure 4. Comparison of PFE for 100-300 nm and 300-750 nm aerosol size bins for selected materials of single and multiple layers, as well as in combination with multiple types of materials.

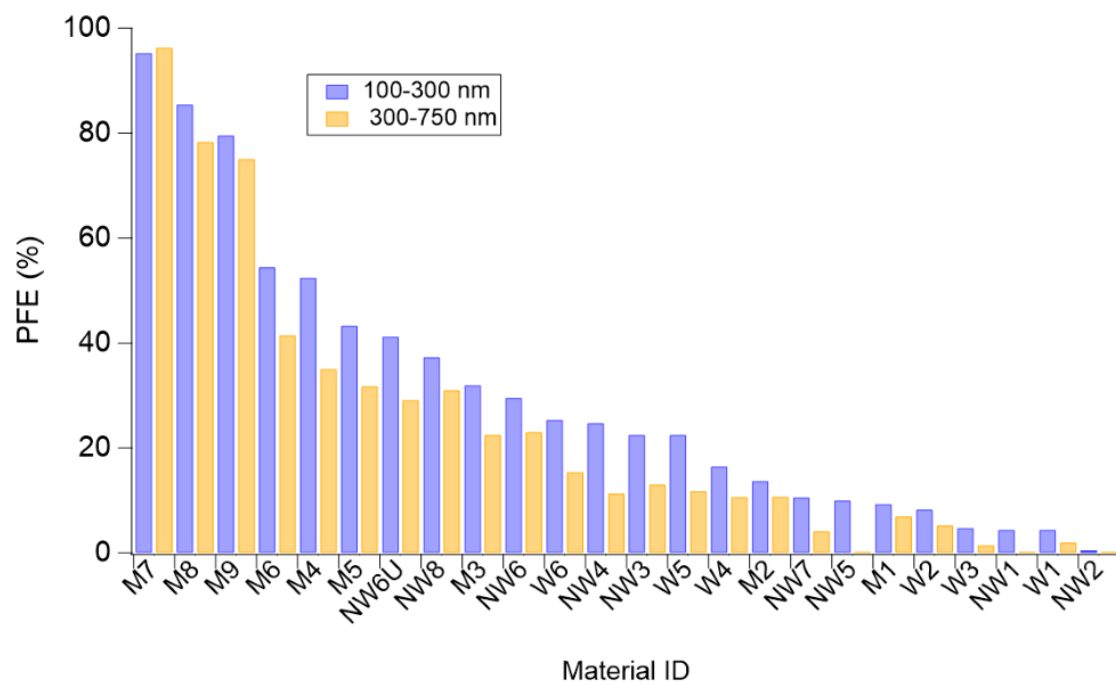


Figure 5. Ranking of PFE for 100-300 nm and 300-750 nm aerosol size bins for all tested materials.

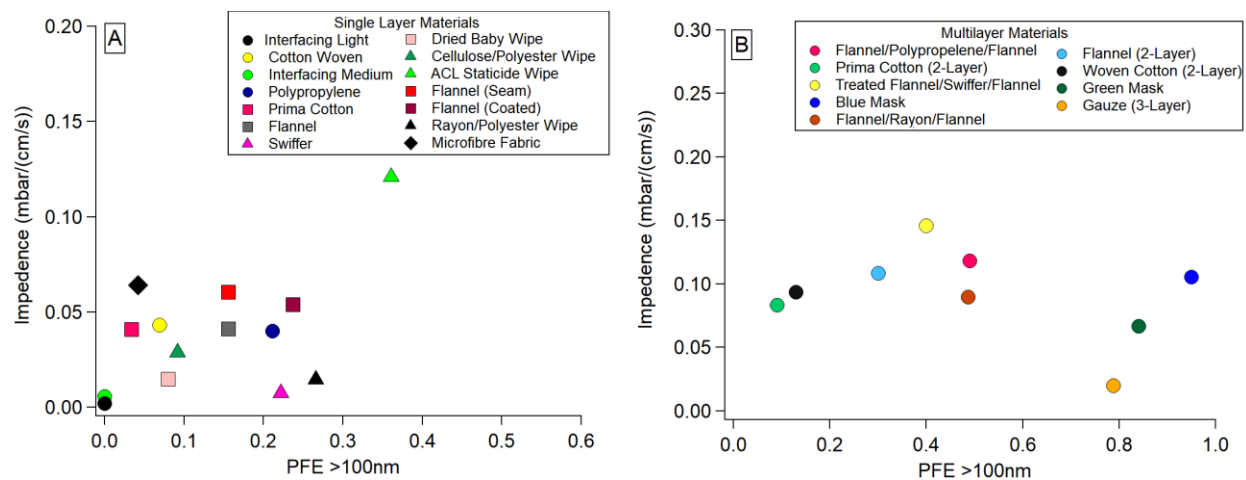


Figure 6. Plots of PFE (>100nm) vs impedance for single layer materials (a) and multilayer material combinations (b).

1 TOC graphic

2 Sub-micron aerosol filtration of non-woven materials and fabric treatments were investigated to
3 provide evidence-based guidelines for enhancing the performance of cloth-based masks. Select
4 low-cost, readily available and easily cut non-woven materials were identified as suitable filter
5 inserts.

